 CMC, vol.52, no.1, pp.53-71, 2016

B-Spline Wavelet on Interval Finite Element Method for Static and Vibration Analysis of Stiffened Flexible Thin Plate

Xing Wei[1,2], Wen Chen[2], Bin Chen[2,3], Bin Chen[1,4], Bin Chen[2], Bin Chen[1]

Abstract: A new wavelet finite element method (WFEM) is constructed in this paper and two elements for bending and free vibration problems of a stiffened plate are analyzed. By means of generalized potential energy function and virtual work principle, the formulations of the bending and free vibration problems of the stiffened plate are derived separately. Then, the scaling functions of the B-spline wavelet on the interval (BSWI) are introduced to discrete the solving field variables instead of conventional polynomial interpolation. Finally, the corresponding two problems can be resolved following the traditional finite element frame. There are some advantages of the constructed elements in structural analysis. Due to the excellent features of the wavelet, such as multi-scale and localization characteristics, and the excellent numerical approximation property of the BSWI, the precise and efficient analysis can be achieved. Besides, transformation matrix is used to translate the meaningless wavelet coefficients into physical space, thus the resolving process is simplified. In order to verify the superiority of the constructed method in stiffened plate analysis, several numerical examples are given in the end.

Keywords: B-spline wavelet on the interval; Wavelet finite element method; Stiffened plate; Bending analysis; Vibration analysis.

1 Introduction

The finite element method (FEM) has been well accepted in numerous industrial areas for structural analysis and simulation [Zienkiewicz and Taylor (2005); Bathe

[1] State Key Laboratory for Manufacturing System Engineering, School of Mechanical Engineering, Xi'an Jiaotong University, Xi'an 710049, PR China
[2] Department of Mechanical and Aerospace Engineering, Case Western Reserve University, Cleveland Ohio 44106, USA
[3] School of Instrument Science and Engineering, Southeast University, Nanjing 210096, PR China
[4] Corresponding author. Tel: +86 29 82667963; fax: +86 29 82663689.
E-mail address: chenxf@mail.xjtu.edu.cn (X.F. Chen)

(1996); Song, Noh, and Choi (2003); Atluri, Gallagher, and Zienkiewicz (1983); Dong, EI-Gizawy, Juhany, and Atluri (2014)]. It has helped many engineers and scholars to promote their work both in design and application. For example, the structural analysis results by FEM helped the engineers to improve their design. It can test the characteristics of the new theoretical achievements or simulate the experimental environment before it is used in experiment or application.

Stiffened plate is a typical structure used in various mechanical equipment and architecture structures. It can enhance the component and can improve the characteristics of the equipment. Therefore, many scholars and engineers spent much energy and time on precise analysis and test of stiffened structures. For example, based on the work of Han and Atluri (2003), Dong and Atluri developed the two-dimensional weakly-singular symmetric galerkin boundary elements for fatigue crack growth analyses in stiffened panels [Dong and Atluri (2012)]. Patel, Bisagni, and Datta (2011) studied the dynamic buckling behavior of laminated composite stiffened cylindrical shell by using ABAQUS. Fenner and Watson (2012) tackled the buckling problem of stiffened plate with filleted junction by three dimensional finite element in order to optimize the fillet radius along the line junction. [Duran, Rodriguez, and Sanhueza (2012)] applied a low order finite element method to analyzing a stiffened plate based on Reissner-Mindlin equations and Timoshenko beams equations. Fernandes and Neto (2014) analyzed stiffened plates composed by beams and slabs with different materials based on boundary element method. [Golmakani and Mehrabian (2014)] studied the elastic large deflection problem of axisymmetric ring-stiffened circular and annular general angle-ply laminated plates by first order shear deformation theory and the dynamic relaxation method. Askari, Saadatnia, Esmailzadeh, and Younesian (2014) investigated the free and forced vibrations of stiffened triangular plate based on Galerkin approach, the energy balance method and the variational approach. Zhu, Chen, Kong, and Zhang (2014) developed a hybrid method combining finite element analysis and energy finite element analysis together to predict the vibrations of stiffened built-up structure. Shi, Kapania, and Dong (2015) developed a finite element method for the static, vibration and buckling behaviors of curvilinearly stiffened plates. Although many achievements have been obtained for stiffened structure analysis, the precision or efficiency is limited. This is because the traditional finite element or hybrid method with the traditional polynomial function or other traditional interpolation function being used to interpolate the solving field cannot achieve multi-scale analysis for high efficiency and precision.

Wavelet finite element method is a new numerical method developed in the last two decades, which takes wavelet functions to replace traditional interpolation in field variables discretion. Due to excellent features of the wavelet function, such as mul-

tiresolution, multi-scale and localization etc., the Wavelet Finite Element Method (WFEM) possesses excellent numerical analysis ability. As an example, [Ko, Kurdila, and Pilant (1995)] constructed Daubechies wavelet finite element method and applied it in 1D and 2D elliptic partial differentiation equations with Neumann boundary conditions in 1995. This paper uncovers the prelude on WFEM. Li and Chen (2014) reviewed the recent development of wavelet numerical method, including wavelet weighted residual method, wavelet finite element method, wavelet boundary method and wavelet meshless method. Mitra constructed the 2-D wavelet spectral finite element method for analysis of wave propagation in an isotropic plate [Mitra and Gopalakrishnan (2006)]. Xiang implemented damage detection through a hybrid method by combining the interval wavelets and wavelet finite element model together [Xiang, Matsumoto, Wang, and Jing (2011)]. Li et al. achieved multiple cracks quantitative identification in a rotor by using wavelet finite element method in forward problem to construct the model of the rotor [Li and Dong (2012)]. Yang analyzed the vibration problem of shell structures by using B-spline wavelet on the interval finite element and general shell theory [Yang, Chen, Li, He, and Miao (2012)]. Zhang, Chen, Yang, Li, and He (2014a) developed a stochastic finite element method based on B-spline wavelet on the interval for static analysis of 1D and 2D structures. Wang and Wu (2013) investigated a new kind of operator-orthogonal wavelet-based element for adaptive analysis of thin plate bending problems. Liu, Xiang, Gao, Jiang, Zhou, and Li (2014) implemented WFEM to analyze the dispersion relation for one dimensional phononic crystals. Yang, Chen, Li, Miao, and He (2014) applied BSWI finite element method for wave motion analysis in arch structures. Xue, Zhang, Li, Qiao, and Chen (2014) proposed a multi-scale wavelet-based numerical method for wave propagation and load identification by introducing modified Hermitian cubic spline wavelets on the interval. Alm, Harbrecht, and Krämer (2014) investigated the fast solution for nonlocal operator equations based on H^2-wavelet method. Zuo et al. studied the static, vibration and buckling problems of functionally graded beams and plates [Zuo, Yang, Chen, Xie, and Zhang (2014a, 2014b)]. Zhao (2015) studied the temperature-pressure coupled field analysis of liquefield petroleum gas tank under jet fire by WFEM. Samaratunga, Jha, and Gopalakrishnan (2015)] developed a wavelet spectral model for studing transient dynamics and wave propagation in adhesively bonded composite joints. In order to improve the calculation precision of generalized stress and strain, [Zhang, Chen, and He (2011a, 2012); Zhang, Chen, He, and Yang (2011b); Zhang, Chen, Yang, and Shen (2014b); Zhang, Zuo, Liu, Chen, and Yang (2016)] constructed a series of multivariable wavelet finite elements for the structures of beam, plate and shell, and static and dynamic characteristics are analyzed and investigated. [Wang, Wu, and Wang (2015)] proposed a design method of second generation wavelet-based multivariable finite element for static and vibration anal-

ysis of beam.

In this paper, the wavelet finite element for stiffened plate is investigated to improve the solving precision and efficiency in bending and free vibration analysis. First, the FEM formulation of the stiffened plate is derived from generalized potential energy function. Then, taking BSWI scaling functions as interpolation function, the solving field variables are discretized. In the meantime, the transformation matrix is constructed to translate the meaningless wavelet coefficients into physical space. Finally, the static and dynamic problems can be resolved by solving the FEM matrix equations.

2 Two-dimensional BSWI

B-spline wavelet on the interval was constructed by Chui and Quak (1992), and the decomposition and reconstruction algorithm was derived in 1994 Quak and Weyrich (1994). The even order BSWI is frequently chosen in practical numerical calculation.

At any scale j, the mth order BSWI scaling functions must satisfy the following condition [Goswami, Chan, and Chui (1995)] in order to have at least one inner wavelet on the interval [0, 1].

$$2^j \geq 2m-1 \tag{1}$$

Since the 0 scale mth order BSWI scaling functions and wavelet functions had been derived by Goswami, Chan, and Chui (1995), the j scale mth order BSWI scaling functions $\phi^j_{m,k}(\xi)$ and wavelet functions $\psi^j_{m,k}(\xi)$ can be evaluated by the following formulas.

$$\phi^j_{m,k}(\xi) = \begin{cases} \phi^l_{m,k}(2^{j-l}\xi), k = -m+1,\ldots,-1 \\ \quad \text{(0 boundary scaling functions)} \\ \phi^l_{m,2^j-m-k}(1--2^{j-l}\xi), k = 2^j-m+1,\ldots,2^j-1 \\ \quad \text{(1 boundary scaling functions)} \\ \phi^l_{m,0}(2^{j-l}\xi-2^{-l}k), k = 0,\ldots,2^j-m \\ \quad \text{(inner boundary scaling functions)} \end{cases} \tag{2}$$

$$\psi^j_{m,k}(\xi) = \begin{cases} \psi^l_{m,k}(2^{j-l}\xi), k = -m+1,\ldots,-1 \\ \quad \text{(0 boundary wavelets)} \\ \psi^l_{m,2^j-2m-k+1}(1--2^{j-l}\xi), k = 2^j-2m+2,\ldots,2^j-m \\ \quad \text{(1 boundary wavelets)} \\ \psi^l_{m,0}(2^{j-l}\xi-2^{-l}k), k = 0,\ldots,2^j-2m+1 \\ \quad \text{(inner wavelets)} \end{cases} \tag{3}$$

The 11 BSWI_{43} scaling functions are given here for the use in the following sections.

$$\phi^3_{4,-3}(\xi)=\frac{1}{6}\times\begin{cases}6-18\times(2^3\xi)+18\times(2^3\xi)^2-6\times(2^3\xi)^3, & \xi\in[0,0.125]\\ 0, & \text{others}\end{cases}$$

$$\phi^3_{4,-2}(\xi)=\frac{1}{6}\times\begin{cases}18\times(2^3\xi)-27\times(2^3\xi)^2+\frac{21}{2}\times(2^3\xi)^3, & \xi\in[0,0.125]\\ 12-18\times(2^3\xi)+9\times(2^3\xi)^2-\frac{3}{2}\times(2^3\xi)^3, & \xi\in[0.125,0.25]\\ 0, & \text{others}\end{cases}$$

$$\phi^3_{4,-1}(\xi)=\frac{1}{6}\times\begin{cases}9\times(2^3\xi)^2-\frac{11}{2}\times(2^3\xi)^3, & \xi\in[0,0.125]\\ -9+27\times(2^3\xi)-18\times(2^3\xi)^2+\frac{7}{2}\times(2^3\xi)^3, & \xi\in[0.125,025]\\ 27-27\times(2^3\xi)9\times(2^3\xi)^2-(2^3\xi)^3, & \xi\in[0.25,0375]\\ 0, & \text{others}\end{cases}$$

$$\phi^3_{4,0}(\xi)=\frac{1}{6}\times\begin{cases}(2^3\xi)^3, & \xi\in[0,0.125]\\ 4-12\times(2^3\xi)+12\times(2^3\xi)^2-3\times(2^3\xi)^3, & \xi\in[0.125,0.25]\\ -44+60\times(2^3\xi)-24\times(2^3\xi)^2+3\times(2^3\xi)^3, & \xi\in[0.25,0.375]\\ 64-48\times(2^3\xi)+12\times(2^3\xi)^2-(2^3\xi)^3, & \xi\in[0.375,0.5]\end{cases}$$

$$\phi^3_{4,1}(\xi)=\phi^3_{4,0}(\xi-0.125),\phi^3_{4,2}(\xi)=\phi^3_{4,0}(\xi-0.25),\phi^3_{4,3}(\xi)=\phi^3_{4,0}(\xi-0.375)$$
$$\phi^3_{4,4}(\xi)=\phi^3_{4,0}(\xi-0.5),\phi^3_{4,5}(\xi)=\phi^3_{4,-1}(1-\xi),\ \phi^3_{4,6}(\xi)=\phi^3_{4,-2}(1-\xi),$$
$$\phi^3_{4,7}(\xi)=\phi^3_{4,-3}(1-\xi)$$

Where, $\phi^3_{4,-3}(\xi)$, $\phi^3_{4,-2}(\xi)$, and $\phi^3_{4,-1}(\xi)$ are 0 boundary scaling functions. $\phi^3_{4,5}(\xi)$, $\phi^3_{4,6}(\xi)$ and $\phi^3_{4,7}(\xi)$ are 1 boundary scaling functions. $\phi^3_{4,0}(\xi)$, $\phi^3_{4,1}(\xi)$, $\phi^3_{4,2}(\xi)$, $\phi^3_{4,3}(\xi)$, and $\phi^3_{4,4}(\xi)$ are inner scaling functions.

The vector form of the BSWI scaling functions is:

$$\boldsymbol{\Phi}=\left\{\phi^j_{m,-m+1}(\xi)\phi^j_{m,-m+2}(\xi)\dots\phi^j_{m,2^j-1}(\xi)\right\} \tag{4}$$

The vector form of BSWI wavelet functions is:

$$\boldsymbol{\Psi}=\left\{\psi^j_{m,-m+1}(\xi)\psi^j_{m,-m+2}(\xi)\dots\psi^j_{m,2^j-m}(\xi)\right\} \tag{5}$$

Two dimensional BSWI can be generated from the BSWI vectors in Eqs. (4–5) by tensor product. The two dimensional BSWI scaling functions are:

$$\boldsymbol{\Phi}=\boldsymbol{\Phi}_1\otimes\boldsymbol{\Phi}_2 \tag{6}$$

where, $\mathbf{\Phi}_1$ and $\mathbf{\Phi}_2$ are BSWI scaling function vector in Eq. (4).

The two dimensional BSWI wavelet functions are:

$$\boldsymbol{\psi}^1 = \mathbf{\Phi}_1 \otimes \boldsymbol{\psi}_2 \tag{7}$$

$$\boldsymbol{\psi}^2 = \boldsymbol{\psi}_1 \otimes \mathbf{\Phi}_2 \tag{8}$$

$$\boldsymbol{\psi}^3 = \boldsymbol{\psi}_1 \otimes \boldsymbol{\psi}_2 \tag{9}$$

where, $\boldsymbol{\psi}_1$ and $\boldsymbol{\psi}_2$ are BSWI wavelet function vector in Eq. (5).

The corresponding two dimensional BSWI scaling functions and wavelet functions are shown in Fig. 1.

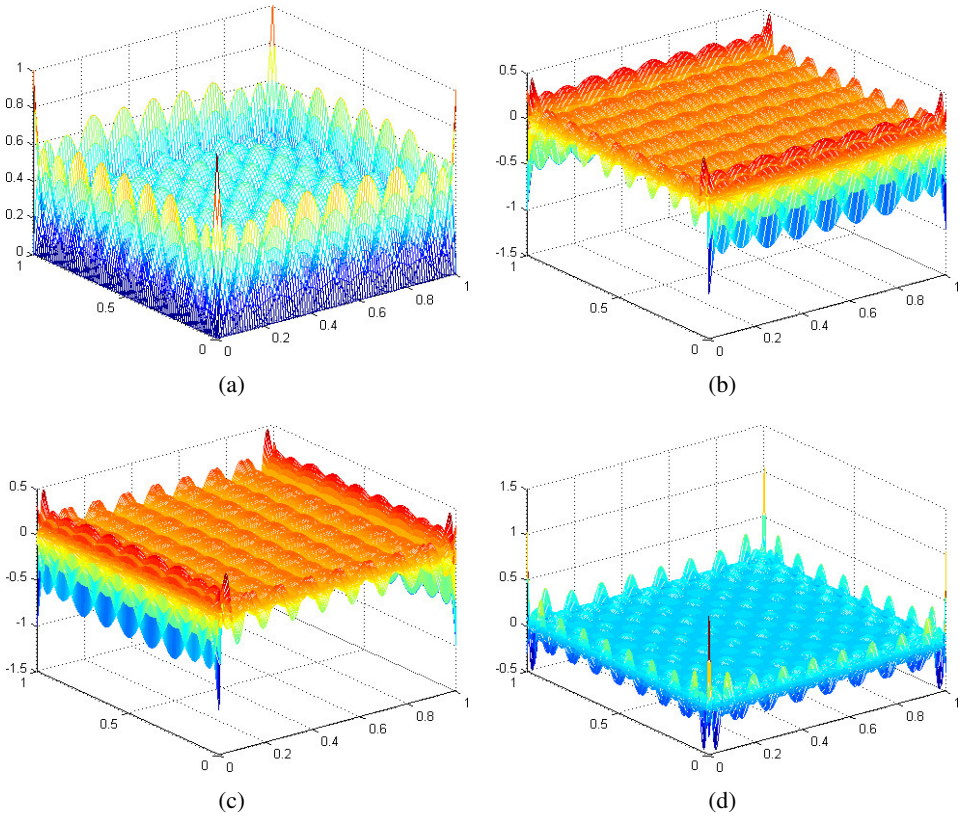

Figure 1: Two dimensional BSWI scaling and wavelet functions. (a) scaling functions $\mathbf{\Phi} = \mathbf{\Phi}_1 \otimes \mathbf{\Phi}_2$ and (b) wavelet functions $\boldsymbol{\psi}^1 = \mathbf{\Phi}_1 \otimes \boldsymbol{\psi}_2$; (c) wavelet functions $\boldsymbol{\psi}^2 = \boldsymbol{\psi}_1 \otimes \mathbf{\Phi}_2$ and (d) wavelet functions $\boldsymbol{\psi}^3 = \boldsymbol{\psi}_1 \otimes \boldsymbol{\psi}_2$.

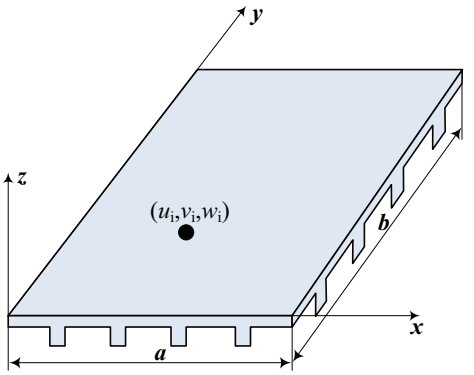

Figure 2: Stiffened plate model and node displacement.

3 BSWI element for bending analysis of stiffened plate

3.1 BSWI element construction

As shown in Fig. 2, there are three Degrees of Freedom (DOF) in each node. The total potential energy of the stiffened flexible thin plate is consisted with strain energy of the flexible thin plate, strain energy of the stiffeners and the potential energy of the load. Therefore, the total potential energy function of the stiffened flexible thin plate can be obtained as Shen (1991):

$$\prod_{\mathrm{p}} = U_{\mathrm{b}} + U_{\mathrm{s}} + \sum_{\mathrm{i}} U_{\mathrm{i}} + \sum_{\mathrm{j}} U_{\mathrm{j}} + V_{\mathrm{p}} \tag{10}$$

where,

U_b is the bending strain energy of the flexible thin plate:

$$U_b = \frac{D}{2} \int_{\Omega} \left[\left(\frac{\partial^2 w}{\partial x^2} \right)^2 + \left(\frac{\partial^2 w}{\partial y^2} \right)^2 + 2\mu \frac{\partial^2 w}{\partial x^2} \cdot \frac{\partial^2 w}{\partial y^2} + 2(1-\mu) \left(\frac{\partial^2 w}{\partial x \partial y} \right)^2 \right] dxdy \tag{11}$$

U_s is the tensile strain energy of the flexible thin plate.

$$U_s = \frac{d}{2} \int_{\Omega} \left[\left(\frac{\partial u}{\partial x} \right)^2 + 2\mu \frac{\partial u}{\partial x} \cdot \frac{\partial v}{\partial y} + \left(\frac{\partial v}{\partial y} \right)^2 + \frac{1-\mu}{2} \left(\frac{\partial u}{\partial y} + \frac{\partial v}{\partial x} \right)^2 \right] dxdy \tag{12}$$

U_i is the strain energy of stiffeners along x direction.

$$U_i = \frac{1}{2} \int_0^a E_i A_i \left(\frac{\partial u_i}{\partial x} \right)^2 dx + \frac{1}{2} \int_0^a E_i I_i \left(\frac{\partial^2 w_i}{\partial x^2} \right)^2 dx + \frac{1}{2} \int_0^a G_i J_i \left(\frac{\partial^2 w_i}{\partial x \partial y} \right)^2 dx \tag{13}$$

U_j is the strain energy of stiffeners along y direction.

$$U_j = \frac{1}{2}\int_0^b E_j A_j \left(\frac{\partial v_j}{\partial y}\right)^2 dy + \frac{1}{2}\int_0^b E_j I_j \left(\frac{\partial^2 w_j}{\partial y^2}\right)^2 dy + \frac{1}{2}\int_0^b G_j J_j \left(\frac{\partial^2 w_j}{\partial x \partial y}\right)^2 dy \quad (14)$$

V_p is the potential energy of load.

$$V_p = \int_\Omega qw dx dy \quad (15)$$

Where, u, v, w are the displacement of flexible thin plate in middle plane along the direction of x, y and z respectively shown in Fig. 2. D is the bending stiffness. μ is poisson ratio. E, E_i and E_j are the elastic modulus of flexible thin plate, stiffeners along x direction and stiffeners along y direction respectively. A_i and A_j are the cross area of the stiffeners along x and y direction. I_i and I_j are the inertia moment of stiffeners along x and y direction. G_i and G_j are the shear modulus of stiffeners along x and y direction. q is the load.

The BSWI scaling function in Eq. (4) is used to discrete the displacement field variables.

$$u = \mathbf{\Phi} T^e u^e \quad (16)$$

$$v = \mathbf{\Phi} T^e v^e \quad (17)$$

$$w = \mathbf{\Phi} T^e w^e \quad (18)$$

where, T^e is the transformation matrix, which can be expressed as follows.

$$T^e = (\mathbf{\Phi}_1 \otimes \mathbf{\Phi}_2)^{-1} \quad (19)$$

$$\begin{cases} \mathbf{\Phi}_1 = \left\{\phi_1^T(\xi_1)\phi_1^T(\xi_2)\ldots\phi_1^T(\xi_{n+1})\right\}^T \\ \mathbf{\Phi}_2 = \left\{\phi_2^T(\eta_1)\phi_2^T(\eta_2)\ldots\phi_2^T(\eta_{n+1})\right\}^T \end{cases} \quad (20)$$

Substituting Eqs. (11–20) into Eq. (10), and based on the minimum potential energy principle, $\frac{\partial \prod_p}{\partial u^e} = 0$, $\frac{\partial \prod_p}{\partial v^e} = 0$ and $\frac{\partial \prod_p}{\partial w^e} = 0$, the BSWI finite element for the stiffened flexible thin plate can be obtained as follows.

$$\begin{bmatrix} K_{11} & K_{12} & K_{13} \\ K_{21} & K_{22} & K_{23} \\ K_{31} & K_{32} & K_{33} \end{bmatrix} \begin{bmatrix} u^e \\ v^e \\ w^e \end{bmatrix} = \begin{bmatrix} 0 \\ 0 \\ (T^e)^T \int_\Omega \Phi_1 \otimes \Phi_2 dx dy \end{bmatrix} \quad (21)$$

where,

$$K_{11} = d\Gamma_1^{11} \otimes \Gamma_2^{00} + \frac{d(1-\mu)}{2}\Gamma_1^{00} \otimes \Gamma_2^{11} + \sum_i E_i A_i \Gamma_1^{11} \otimes \Gamma_2^{00};$$

$$K_{12} = d\mu\Gamma_1^{10} \otimes \Gamma_2^{01} + \frac{d(1-\mu)}{2}\Gamma_1^{01} \otimes \Gamma_2^{10};$$

$$K_{13} = -\sum_i E_i A_i e_i \Gamma_1^{12} \otimes \Gamma_2^{00};$$

$$K_{21} = (K_{12})^T;$$

$$K_{22} = d\Gamma_1^{00} \otimes \Gamma_2^{11} + \frac{d(1-\mu)}{2}\Gamma_1^{11} \otimes \Gamma_2^{00} + \sum_j E_j A_j \Gamma_1^{00} \otimes \Gamma_2^{11};$$

$$K_{23} = -\sum_j E_j A_j e_j \Gamma_1^{00} \otimes \Gamma_2^{12};$$

$$K_{31} = (K_{13})^T;$$

$$K_{32} = (K_{23})^T;$$

$$\begin{aligned} K_{33} = {} & D\Gamma_1^{22} \otimes \Gamma_2^{00} + D\Gamma_1^{00} \otimes \Gamma_2^{22} + \mu D\Gamma_1^{20} \otimes \Gamma_2^{02} + \mu D\Gamma_1^{02} \otimes \Gamma_2^{20} \\ & + 2D(1-\mu)\Gamma_1^{11} \otimes \Gamma_2^{11} + \sum_i E_i A_i e_i^2 \Gamma_1^{22} \otimes \Gamma_2^{00} + \sum_i E_i I_j \Gamma_1^{22} \otimes \Gamma_2^{00} \\ & + \sum_i G_i J_j \Gamma_1^{11} \otimes \Gamma_2^{11} + \sum_j E_j A_j e_j^2 \Gamma_1^{00} \otimes \Gamma_2^{22} + \sum_j E_j I_i \Gamma_1^{00} \otimes \Gamma_2^{22}. \\ & + \sum_j G_j J_j \Gamma_1^{11} \otimes \Gamma_2^{11} \end{aligned}$$

where the integral terms are:

$$\mathbf{\Gamma}_1^{00} = (T^e)^T L_x \int_0^1 \mathbf{\Phi}_1^T \mathbf{\Phi}_1 d\xi T^e;$$

$$\mathbf{\Gamma}_1^{10} = (T^e)^T \int_0^1 \frac{d\mathbf{\Phi}_1^T}{d\xi} \mathbf{\Phi}_1 d\xi T^e;$$

$$\mathbf{\Gamma}_1^{01} = (\mathbf{\Gamma}_1^{10})^T;$$

$$\mathbf{\Gamma}_1^{20} = (T^e)^T \frac{1}{L_x} \int_0^1 \frac{d^2\mathbf{\Phi}_1^T}{d\xi^2} \mathbf{\Phi}_1 d\xi T^e;$$

$$\mathbf{\Gamma}_1^{02} = (\mathbf{\Gamma}_1^{20})^T.$$

Substituting L_x and $d\xi$ as L_y and $d\eta$ in $\mathbf{\Gamma}_1^{i,j}(i,j=0,1,2)$, the expression of $\mathbf{\Gamma}_2^{i,j}(i,j=0,1,2)$ can be obtained.

3.2 Numerical examples

3.2.1 Bending analysis example 1

As shown in Fig. 3, the clamped flexible thin plate with two orthogonal stiffeners is considered in this numerical example for bending analysis. The corresponding parameters of this plate are: Elastic modulus $E = 2.116 \times 10^4$ N/mm; Poisson ratio $\mu = 0.3$; Plate length $a = b = 201.8$ mm; Plate thickness $t = 2.817$ mm; Distributed load $q = 0.005$ N/mm^2. The parameters of the two stiffeners are: Moment of inertia $I = 59.6$ mm^4; Offset $e = 0$.

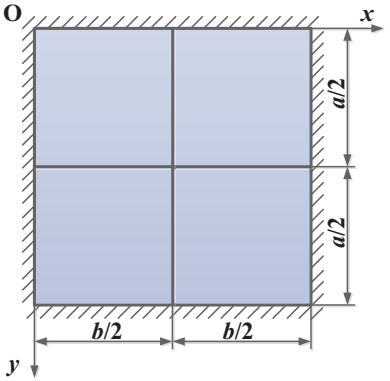

Figure 3: Clamped flexible thin plate with two orthogonal stiffeners.

Table 1: Displacement and moment of the stiffened flexible plate with two orthogonal stiffeners.

	w(mm)			M(N · mm)		
x/b (y/a =1/2)	Spline FEM	BSWI FEM	Experiment	Spline FEM	BSWI FEM	Experiment
0	0	0	0	7.452	7.5832	7.927
1/10	/	0.02803	/	/	3.1493	/
1/8	0.040695	0.04088	0.049	1.6686	1.4288	/
2/10	/	0.08438	/	/	0.3122	/
2/8	0.112957	0.01142	0.117	1.7812	1.6632	/
3/10	/	0.14013	/	/	2.3419	/
3/8	0.16899	0.16918	0.169	3.2989	3.1825	/
4/10	/	0.17648	/	/	3.3226	/
1/2	0.18901	0.18919	0.185	3.60887	3.5731	3.379

The static bending problem of the stiffened flexible thin plate with two orthogonal stiffeners clamped with distributed load is analyzed in this example. The displace-

ment of middle plane and moment results are compared with spline FEM [Shen, Huang, and Wang (1987)], BSWI FEM and experimental results [Shen (1991)] in Table 1. $BSWI_{43}$ is used to discrete the displacement field variables, so there are 363 DOFs in each BSWI element. The results of these three elements are in consistent with each other, so the correctness of the proposed BSWI FEM is verified. With a relatively small computational cost, it can achieve similar precision as spline FEM and experiment do. Besides, the isolines and global deformation in Fig. 4 further demonstrated that the analyzed results are reasonable. Therefore, the constructed BSWI FEM is an efficient way in bending analysis for stiffened flexible thin plate.

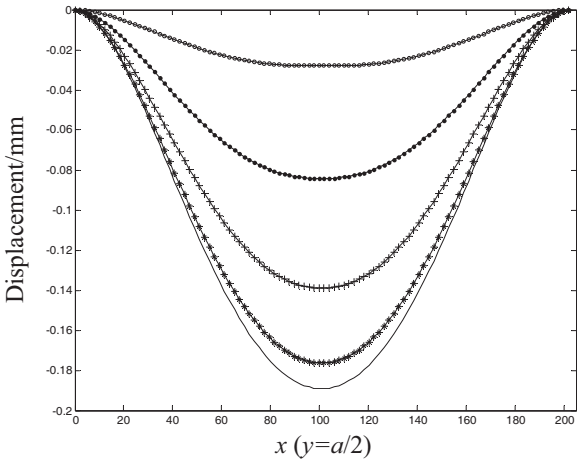

Figure 4: Deformation of the stiffened flexible thin plate with two orthogonal stiffeners (Isoline along $y = a/2$).

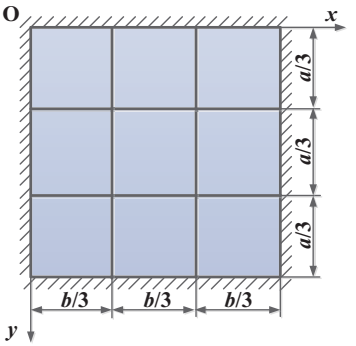

Figure 5: Clamped flexible thin plate with four orthogonal stiffeners.

3.2.2 Bending analysis example 2

As shown in Fig. 5, the square stiffened flexible thin plate with four orthogonal stiffeners is considered in this example. The corresponding parameters are: Elastic modulus $E = 2.116 \times 10^4$ N/mm; Poisson ratio $\mu = 0.3$; Plate length $a = b = 201.8$ mm; Plate thickness $t = 2.817$ mm; Distributed load $q = 0.005$ N/mm^2. The parameters of the four stiffeners are: Moment of inertia $I = 45.0702$ mm^4; Offset $e = 0$.

The bending problem of the stiffened flexible thin plate with four orthogonal stiffeners is analyzed in this numerical example. The displacement of middle plane and moment results are shown in Table 2 and the deformation of the stiffened thin plate

Table 2: Displacement and moment of the stiffened flexible plate with four orthogonal stiffeners.

		w(mm)			M(N·cm)		
y/a	x/b	Spline FEM	BSWI FEM	Experiment	Spline FEM	BSWI FEM	Experiment
	0	0	0	0	7.8303	7.7821	8.2301
	1/10	/	0.02931	/	/	3.3485	/
	1/8	0.04223	0.04352	0.044	1.20787	1.9524	/
	2/10	/	0.08831	/	/	0.5768	/
1/2	2/8	0.11495	0.11522	0.114	1.89021	1.8232	/
	3/10	/	0.14485	/	/	2.5159	/
	3/8	0.17219	0.17328	0.1660	3.37769	3.3540	/
	4/10	/	0.18511	/	/	3.5344	/
	1/2	0.19365	0.19687	0.1840	4.0375	3.9421	3.491

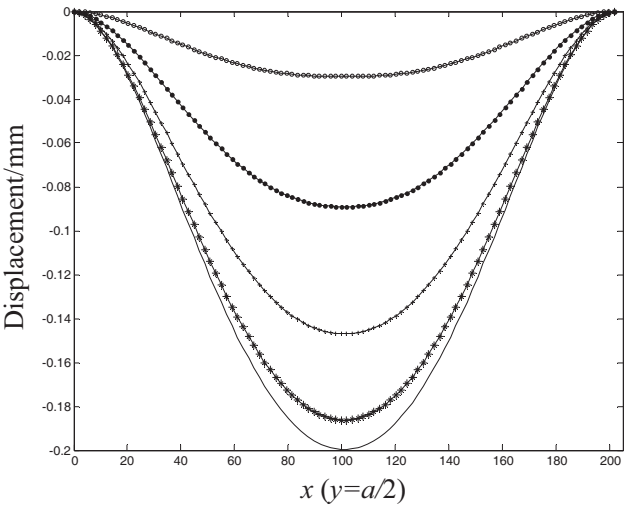

Figure 6: Deformation of the stiffened flexible thin plate with four orthogonal stiffeners (Isoline along $y = a/2$).

are drawn in Fig. 6. It can be seen from the comparison among spline FEM [Shen (1991)], BSWI FEM and experiment [Shen (1991)] in Table 2 that the results of the three methods are in consistent with other. For BSWI FEM, only one element is used in this example, so the proposed BSWI FEM is an efficient way in structural analysis. Besides, the global deformation and isolines in Fig. 6 further demonstrate the correctness of the BSWI FEM.

4 Bswi element for free vibration analysis of stiffened plate

4.1 BSWI element construction

The total potential energy of the stiffened flexible thin plate in Fig. 2 is [Shen (1991)]:

$$\prod_p = \frac{1}{2}\Delta^T K\Delta - \frac{1}{2}\omega^2\Delta^T M\Delta \tag{22}$$

Where, $\Delta = [u \;\; v \;\; w]$ is the displacement in middle plane.

According to minimum potential energy principle $\dfrac{\partial \prod_p}{\partial \Delta} = 0$,

$$\left(K - \omega^2 M\right)\Delta = 0 \tag{23}$$

the frequency equation to free vibration can also be obtained.

$$\left|K - \omega^2 M\right| = 0 \tag{24}$$

By solving the frequency equation in Eq. (24), the natural frequencies ω and corresponding mode shapes can be obtained.

K can be solved and obtained as shown in section 3.1, so the next problem is how to get M.

The maximum kinetic energy of the stiffened flexible thin plate is:

$$V = \omega^2 T \tag{25}$$

where,

$$T = \frac{1}{2}\int_{\Omega} \bar{m}\left(u^2 + v^2 + w^2\right)\mathrm{d}x\mathrm{d}y + \frac{1}{2}\sum\int\left[\bar{m}_i\left(u_i^2 + v_i^2 + w_i^2\right) + J_i\left(\frac{\partial w_i}{\partial x}\right)^2\right]\mathrm{d}y$$
$$+ \frac{1}{2}\sum\int\left[\bar{m}_j\left(u_j^2 + v_j^2 + w_j^2\right) + J_j\left(\frac{\partial w_j}{\partial y}\right)^2\right]\mathrm{d}x = \frac{1}{2}\Delta^T M\Delta \tag{26}$$

where, $\bar{m}$, $\bar{m}_i$ and $\bar{m}_j$ are the density of thin plate and ribs along x and y directions. ω is circular frequency. Other symbols are the same as those in Eq. (10).

Then, according to Eq. (25), the mass matrix for vibration problem of the stiffened flexible thin plate can be obtained.

$$M = \begin{bmatrix} M_{11} & M_{12} & M_{13} \\ M_{21} & M_{22} & M_{23} \\ M_{31} & M_{32} & M_{33} \end{bmatrix} \tag{27}$$

where,

$$
\begin{aligned}
M_{11} &= \bar{m}\Gamma_1^{00}\otimes\Gamma_2^{00}+\sum\bar{m}_i\Gamma_1^{00}\otimes\Gamma_2^{00}+\sum\bar{m}_j\Gamma_1^{00}\otimes\Gamma_2^{00};\\
M_{12} &= 0;\\
M_{13} &= -\sum\bar{m}_i e_i\Gamma_1^{01}\otimes\Gamma_2^{01}-\sum\bar{m}_j e_j\Gamma_1^{01}\otimes\Gamma_2^{00};\\
M_{21} &= (M_{12})^T;\\
M_{22} &= \bar{m}\Gamma_1^{00}\otimes\Gamma_2^{00}+\sum\bar{m}_i\Gamma_1^{00}\otimes\Gamma_2^{00}+\sum\bar{m}_j\Gamma_1^{00}\otimes\Gamma_2^{00};\\
M_{23} &= -\sum\bar{m}_i e_i\Gamma_1^{00}\otimes\Gamma_2^{01}-\sum\bar{m}_j e_j\Gamma_1^{00}\otimes\Gamma_2^{01};\\
M_{31} &= (M_{13})^T;\\
K_{32} &= (K_{23})^T;\\
M_{33} &= \bar{m}\Gamma_1^{00}\otimes\Gamma_2^{00}+\sum\bar{m}_i\Gamma_1^{00}\otimes\Gamma_2^{00}+\sum\bar{m}_j\Gamma_1^{00}\otimes\Gamma_2^{00}+\sum\bar{m}_i e_i^2\Gamma_1^{00}\otimes\Gamma_2^{11}\\
&\quad+\sum\left(\bar{m}_i e_i^2+J_i\right)\Gamma_1^{00}\otimes\Gamma_2^{00}+\sum\bar{m}_j e_j^2\Gamma_1^{11}\otimes\Gamma_2^{00}+\sum\left(\bar{m}_j e_j^2+J_j\right)\Gamma_1^{00}\otimes\Gamma_2^{11}.
\end{aligned}
$$

The integral terms above are the same as those in section 3.1.

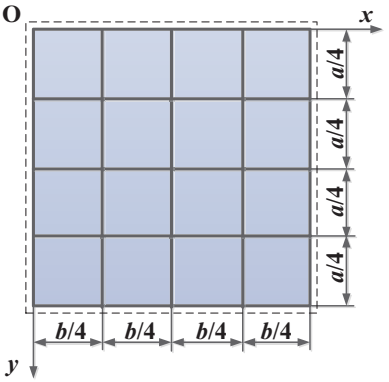

Figure 7: Simply supported flexible thin plate with six orthogonal stiffeners.

4.2 Numerical example

As shown in Fig. 7, the square stiffened flexible thin plate with six orthogonal stiffeners is considered in this numerical example for free vibration analysis. The corresponding material parameters of the plate are: Elastic modulus $E = 10920$; Poisson ratio $\mu = 0.3$; Plate length $a = b = 1$; Plate thickness $t = 0.1$; Bending stiffness $D = 1$; Density $\bar{m} = 1$. The parameters of the eight stiffeners are: Cross area $A = 0.03$; Moment of inertia $I = 0.00025$; Offset $e = 0$.

The free vibration analysis results of simply supported stiffened flexible thin plate are shown in Table 3. The first four circular frequencies are compared with spline FEM [Shen, Huang, and Wang (1987)], BSWI FEM, orthotropic plate [Shen (1991)] and Reference [Cao (1983)]. It can be seen from the comparison that the precision of the constructed BSWI FEM is in consistent with other three methods, while only one BSWI element is used in this free vibration analysis. Therefore, the proposed BSWI FEM is an efficient way in structural analysis, including bending analysis and vibration analysis, which can achieve the results with good precision and small computational cost.

Table 3: Free vibration analysis results of simply supported stiffened flexible thin plate.

	ω_1(rad/s)	ω_2(rad/s)	ω_3(rad/s)	ω_4(rad/s)
Spline FEM	86.0581	247.659	247.659	345.491
BSWI FEM	86.8538	248.9235	248.9235	347.8416
Orthotropic plate	86.0643	246.956	246.956	346.032
Reference	87.3056	250.195	250.195	349.222

5 Conclusion

Based on generalized potential energy function and B-spline wavelet on the interval, a novel BSWI finite element method is constructed for static and free vibration analysis of the stiffened flexible thin plate in this paper. The FEM formulations are derived from the generalized potential energy function according to generalized potential energy function and virtual work principle. BSWI is used to replace polynomial interpolation function in traditional FEM to discrete the solving field variables, and the transformation matrix is constructed to transfer the meaningless wavelet coefficients into physical space. Due to the excellent features of BSWI, the efficient and precise analysis results can be obtained. Through several numerical analysis examples, it proved that the proposed BSWI FEM can achieve static and vibration analysis with high efficiency and precision.

Acknowledgement: This work was supported by the National Natural Science Foundation of China (Nos. 51405370&51421004), the National Key Basic Research Program of China (No. 2015CB057400), the project supported by Natural Science Basic Plan in Shaanxi Province of China (No. 2015JQ5184), the Fundamental Research Funds for the Central Universities (xjj2014014), and Shaanxi Province Postdoctoral Research Project.

References

Alm, D.; Harbrecht, H.; Krämer, U. (2014): The H^2-wavelet method. *Journal of Computational and Applied Mathematics*, vol. 267, pp. 131–159.

Askari, H.; Saadatnia, Z.; Esmailzadeh, E.; Younesian, D. (2014): Multi-frequency excitation of stiffened triangular plates for large amplitude oscillations. *Journal of Sound and Vibration*, vol. 333, pp. 5817–5835.

Atluri, S. N.; Gallagher, R.H.; Zienkiewicz, O. C. (1983): Hybrid and mixed finite element methods. Wiley.

Bathe, K. J. (1996): Finite element procedures. Prentice Hall Press.

Cao, G. X. (1983): Vibration of elastic rectangular plate. China Architecture & Building Press, Beijing.

Chui, C. K.; Quak, E. (1992): Wavelets on a bounded interval. *Numerical Methods of Approximation Theory*, vol. 1, pp. 53–57.

Dong, L. T.; Atluri, S. N. (2012): SGBEM (Using non-hyper-singular traction BIE), and super elements, for non-collonear fatigue-growth analyses of cracks in stiffened panels with composite-patch repairs. *CMES-Computer Modeling in Engineering and Sciences*, vol. 89, pp. 415–456.

Dong, L. T.; EI-Gizawy, A. S.; Juhany, K. A.; Atluri, S. N. (2014): A simple locking-alleviated 4-node mixed-collocation finite element with over-integration, for homogeneous or functionally-graded or thick-section laminated composite beamsplates and shells, with & without Z-pins. *CMC: Computers Materials and Continua*, vol. 41, pp. 163–192.

Duran, R.; Rodriguez, R.; Sanhueza, F. (2012): A finite element method for stiffened plates. *Mathematical Modelling and Numerical Analysis*. vol. 46, pp. 291–315.

Fenner, P. E.; Watson, A. (2012): Finite element buckling analysis of stiffened plates with filleted junctions. *Thin-Walled Structures*, vol. 59, pp. 171–180.

Fernandes, G. R.; Neto, J. R. (2014): Analysis of stiffened plates composed by different materials by boundary element method. *Structural Engineering and Mechanics*, vol. 56, pp. 605–623.

Golmakani, M. E.; Mehrabian, M. (2014): Nonlinear bending analysis of ring-stiffened circular and annular general angle-ply laminated plates with various boundary conditions. *Mechanics Research Communications*, vol. 59, pp. 42–50.

Goswami, J. C.; Chan, A. K.; Chui, C. K. (1995): On solving first-kind integral equations using wavelets on a bounded interval. *IEEE Transactions on Antennas and Propagation*, vol. 43, pp. 614–622.

Han, Z. D.; Atluri, S. N. (2003): Truly meshless Local Petrov-Galerkin (MLPG) solutions of traction & displacement BIEs. *CMES-Computer Modeling in Engineering and Sciences*, vol. 4, pp. 665–678.

Ko, J.; Kurdila, A. J.; Pilant, M. S. (1995): A class of finite element methods based on orthonormal, compactly supported wavelets. *Computational Mechanics*, vol. 16, pp. 235–244.

Li, B.; Chen X. (2014): Wavelet-based numerical analysis: a review and classification. *Finite Elements in Analysis and Design*, vol. 81, pp. 14–31.

Li, B.; Dong, H. (2012): Quantitative identification of multiple cracks in a rotor utilizing wavelet finite element method. *CMES-Computer Modeling in Engineering and Sciences*, vol. 84, pp. 205–228.

Liu, M.; Xiang, J.; Gao, H.; Jiang, Y.; Zhou, Y.; Li, F. (2014): Research on band structure of one-dimensional phononic crystals based on wavelet finite element method. *CMES: Computer Modeling in Engineering & Sciences*, vol. 97, pp. 425–436.

Mitra, M.; Gopalakrishnan, S. (2006): Wavelet based 2-D spectral finite element formulation for wave propagation analysis in isotropic plate. *CMES: Computer Modeling in Engineering and Sciences*, vol. 15, pp. 49–68.

Patel, S. N.; Bisagni, C.; Datta, P. K. (2011): Dynamic buckling analysis of a composite stiffened cylindrical shell. *Structural Engineering and Mechanics*, vol. 37, pp. 509–527.

Quak, E.; Weyrich, N. (1994): Decomposition and reconstruction algorithms for spline wavelets on a bounded interval. *Applied and Computational Harmonic Analysis*, vol. 1, pp. 217–231.

Samaratunga, D.; Jha, R.; Gopalakrishnan, S. (2015): Wave propagation analysis in adhesively bonded composite joints using the wavelet spectral finite element method. *Composite Structures*, vol. 122, pp. 271–283.

Shen, P. (1991): Spline finite methods in structural analysis. Hydraulic and Electric Press, Beijing.

Shen, P.; Huang, D.; Wang, Z. (1987): Static vibration and stability analysis of stiffened plates using B spline functions. *International Journal of Computers and Structures*, vol. 27, pp. 73–78.

Shi, P.; Kapania, R. K.; Dong, C. Y. (2015): Vibration and buckling analysis of curvilinearly stiffened plates using finite element method. *AIAA Journal*, vol. 52, pp. 1319–1335.

Song, M. K.; Noh, H. C.; Choi, C. K. (2003): A new three-dimensional finite element analysis model of high speed train-bridge interactions. *Engineering Structures*, vol. 25, pp. 1611–1626.

Wang, Y.; Wu, Q. (2013): Construction of operator-orthogonal wavelet-based elements for adaptive analysis of thin plate bending problems. *CMES: Computer Modeling in Engineering & Sciences*, vol. 93, pp. 17–45.

Wang, Y.; Wu, Q.; Wang, W. (2015): The construction of second generation wavelet-based multivariable finite elements for multiscale analysis of beam problems. *Structural Engineering and Mechanics*, vol. 50, pp. 679–695.

Xiang, J.; Matsumoto, T.; Wang, Y.; Jing, Z. (2011): A hybrid of interval wavelets and wavelet finite element model for damage detection in structures. *CMES: Computer Modeling in Engineering & Sciences*, vol. 81, pp. 269–294.

Xue, X.; Zhang, X.; Li, B.; Qiao, B.; Chen, X. (2014): Modified Hermitian cubic spline wavelet on interval finite element for wave propagation and load identification. *Finite Elements in Analysis and Design*, vol. 91, pp. 48–58.

Yang, Z.; Chen, X.; Li, B.; He, Z.; Miao, H. (2012): Vibration analysis of curved shell using B-spline wavelet on the interval (BSWI) finite elements method and general shell theory. *CMES: Computer Modeling in Engineering & Science*, vol. 85, pp. 129–156.

Yang, Z.; Chen, X.; Li, X.; Miao, H.; He, Z. (2014): Wave motion analysis in arch structures via wavelet finite element method. *Journal of Sound and Vibration*, vol. 333, pp. 446–469.

Zhang, X.; Chen, X.; He, Z. (2011a): The construction of multivariable Reissner-Mindlin plate elements based on B-spline wavelet on the interval. *Structural Engineering and Mechanics*, vol. 38, pp. 733–751.

Zhang, X.; Chen, X.; He, Z. (2012): The multivariable finite elements based on B-spline wavelet on the interval for 1D structural mechanics. *Journal of Vibroengineering*, vol. 14, pp. 363–380.

Zhang, X.; Chen, X.; He, Z.; Yang, Z. (2011b): The analysis of shallow shells based on multivariable wavelet finite element method. *Acta Mechanica Solida Sinica*, vol. 24, pp. 450–460.

Zhang, X.; Chen, X.; Yang, Z.; Li, B.; He, Z. (2014a): A stochastic wavelet finite element method for 1D and 2D structures analysis. *Shock and Vibration*, vol. 2014, no. 104347.

Zhang, X.; Chen, X.; Yang, Z.; Shen, Z. (2014b): Multivariable wavelet finite element for flexible skew thin plate analysis. *Science China Technological Sciences*, vol. 57, pp. 1532–1540.

Zhang, X.; Zuo, H.; Liu, J.; Chen, X.; Yang, Z. (2016): Analysis of shallow hyperbolic shell by different kinds of wavelet elements based on B-spline wavelet on the interval. *Applied Mathematical Modelling*, vol. 40, pp. 1914–1928.

Zhao, B. (2015): The application of super wavelet finite element on temperature-pressure coupled field simulation of LPG tank under jet fire. *Heat and Mass Transfer*, vol. 51, pp. 231–237.

Zhu, D.; Chen, H.; Kong, X.; Zhang, W. (2014): A hybrid finite element-energy finite element method for mid-frequency vibrations of built-up structures under multi-distributed loadings. *Journal of Sound and Vibration*, vol. 333, pp. 5723–5745.

Zienkiewicz, O. C.; Taylor, R. L. (2005): The finite element method for solid and structural mechanics, 6^{th} edition. Elsevier Press.

Zuo, H.; Yang, Z.; Chen, X.; Xie, Y. Zhang, X.; Liu, Y.(2014a): Static, free vibration and buckling analysis of functionally graded beam via B-spline wavelet on the interval and Timoshenko beam theory. *CMES-Computer Modeling in Engineering & Sciences*, vol. 100, pp. 477–506.

Zuo, H.; Yang, Z.; Chen, X.; Xie, Y.; Zhang, X. (2014b): Bending, free vibration and buckling analysis of functionally graded plates via wavelet finite element method. *CMC-Computers Materials and Continua*, vol. 44, pp. 167–204.